A Hybrid Model Integrating Interval Type-2 Fuzzy Logic (IT2FL) and XGBoost for Enhanced Prostate Cancer Analytics

Umoh A. Uduak[1], Udoinyang G. Inyang[2], Blessing E., Akponome[4], Emmanuel A. Ubong[3]

[1]Department of Information Systems, Faculty of Computing, University of Uyo, Nigeria

[2]Department of Data Science, Faculty of Computing, University of Uyo, Nigeria

[3]School of Computing and Information Technology, Federal University of Technology, Ikot Abasi. Nigeria

[4] Computer Science, Nigeria Maritime University, Okerenkoko, Delta, Nigeria

DOI: https://doi.org/10.68050/JAMS.2026.741

Received: 20 October 2026; Accepted: 28 October 2026; Published: 04 November 2026

ABSTRACT

Diagnosing prostate cancer continues to be difficult because of the drawbacks related to traditional methods like PSA testing and digital rectal examination, which can yield false positives, false negatives, and subjective results. These issues may lead to avoidable biopsies and postponed recognition of high-risk situations. This research introduces a hybrid diagnostic framework that combines eXtreme Gradient Boosting (XGBoost) with Interval Type-2 Fuzzy Logic (IT2FL) to tackle uncertainty in assessing prostate cancer risk. The IT2FL component represents uncertainty in clinical information with linguistic rules and assesses three primary factors: Age, Family History, and Race (African Ancestry) using 18 fuzzy rules defined by experts to produce a binary risk classification (Yes/No). The resulting representations are then handled by XGBoost for the final classification. The evaluation of performance on 5,589 test samples resulted in a total accuracy of 0.97. For the No class, the model reached a precision of 0.97, a recall of 0.83, and an F1-score of 0.89, whereas the Yes class attained a precision of 0.96, a recall of 0.99, and an F1-score of 0.98. The macro-average precision, recall, and F1-score were 0.97, 0.91, and 0.94, respectively, while the weighted-average F1-score stood at 0.96. An evaluation of the case with Age = 52, Family History = 0, and Race = 1 further illustrated the model's use in personal risk categorization. The results show that the IT2FL-XGBoost framework delivers classified capabilities while maintaining the clarity of fuzzy reasoning, highlighting its potential as a decision-support method for assessing prostate cancer risk.

Keywords: Prostate Cancer, IT2FL, Machine Learning, XGBoost, Feature Selection, Healthcare, Prognosis

1.0 INTRODUCTION

Prostate cancer (PCa) is a significant worldwide health issue and ranks as one of the most commonly diagnosed cancers in men. In the United States, 268,490 new cases and 34,500 fatalities were projected in 2022, whereas in Nigeria, advanced-stage diagnosis leads to significant mortality (Siegel et al., 2022; Iheanacho and Enechukwu, 2024). The weight is especially significant among men of African descent, who tend to face greater PCa rates and death than many other groups (DeSantis et al., 2019). These differences underscore the necessity for trustworthy methods that facilitate earlier detection of risks.

Traditional PCa evaluation depends on prostate-specific antigen (PSA), digital rectal examination (DRE), clinical background, and biopsy. While PSA enhanced early diagnosis, its restricted specificity can lead to false positives, unnecessary biopsies, overdiagnosis, and overtreatment, whereas DRE is still subjective and might overlook non-palpable tumors (Negoita et al., 2018; Siegel et al., 2020). Biopsies guided by TRUS may also result in sampling inaccuracies. Improvements in multiparametric MRI and biomarkers have enhanced lesion characterization and risk evaluation; however, their expenses, technical demands, and interpretative

inconsistencies may restrict accessibility, especially in resource-limited environments (Kohaar et al., 2019; Leyh-Bannurah et al., 2019). Machine learning (ML) offers a different approach for detecting nonlinear associations and intricate patterns in clinical data. Among ensemble techniques, eXtreme Gradient Boosting (XGBoost) has shown considerable predictive power for organized medical data (Lundervold and Lundervold, 2019). Nevertheless, traditional ML models might offer a restricted depiction of the uncertainty and imprecision present in clinical variables. Fuzzy logic overcomes this constraint by utilizing linguistic variables and rule-based reasoning to represent information. Interval Type-2 Fuzzy Logic (IT2FL) enhances membership functions by integrating uncertainty via a Footprint of Uncertainty, which renders it appropriate for vague clinical data and expert insights (Umoh et al., 2019; Umoh et al., 2020; Ge et al., 2023; Pandey et al., 2023).

Even with progress in ML and fuzzy-based medical decision support, there has been little integration of uncertainty-aware IT2FL reasoning with XGBoost for prostate cancer risk classification utilizing interpretable clinical predictors. This research thus introduces an IT2FL–XGBoost framework that combines Age, Family History, and Race (African Ancestry) using 18 expert-defined fuzzy rules to create a comprehensible risk representation, later analyzed by XGBoost for binary Yes/No classification. The framework is assessed through precision, recall, F1-score, accuracy, and metrics for specific class performance. The research seeks to merge the uncertainty depiction and interpretability of IT2FL with the nonlinear predictive power of XGBoost, offering a computational decision-support method for PCa risk evaluation that enhances traditional clinical diagnosis.

2.0 RELATED WORKS

2.1 AI Applications and Histopathology

Artificial Intelligence (AI), particularly machine learning, is revolutionizing radiology by automating tasks traditionally dependent on human expertise. In prostate cancer (PCa) diagnosis, AI enhances detection, staging, and treatment planning. Convolutional neural networks (CNNs) are widely applied for MRI image analysis, aiding segmentation, biopsy targeting, and 3D tumor visualization, though human validation remains essential (Taye et al., 2023). Studies show AI can match or exceed radiologist accuracy, especially in standardized systems like PI-RADS (Cuocolo et al., 2021). Beyond PCa, AI demonstrates strong diagnostic capabilities, such as achieving over 83% precision in appendicitis classification (Chervenkov et al., 2023). When integrated with clinical factors—PSA levels, biopsy history AI supports risk stratification, reducing unnecessary biopsies and guiding aggressive cancer detection (Bhattacharya et al., 2022). It also improves consistency in biopsy grading, minimizing inter-observer variability. Despite MRI being the most effective non-invasive tool, interpretation challenges persist due to subtle tissue differences and false positives (Liu et al., 2018; Turkbey et al., 2019; Ahmed et al., 2017). Emerging AI models address these limitations and predict disease progression and recurrence, enabling personalized care and better outcomes (Wang et al., 2021; Hiremath et al., 2021).

2.2 Importance of accurate prognosis in treatment planning

Accurate prognosis is critical in prostate cancer treatment planning as it guides the selection of the most effective therapy. A precise assessment enables clinicians to tailor interventions based on cancer stage, patient health, and anticipated response, improving treatment outcomes while minimizing side effects. By predicting disease progression, healthcare providers can decide whether surgery, radiation, hormone therapy, or a combination is appropriate. Conversely, inaccurate prognosis risks overtreatment or undertreatment, leading to unnecessary toxicity or inadequate cancer control. Ultimately, reliable prognostic information optimizes treatment decisions, enhances survival rates, and preserves quality of life for patients.

2.3 The Role of Hybrid Systems in Medical Diagnosis

Recent healthcare advancements have been driven by emerging technologies that enhance medical systems (Paul et al., 2023). Technologies such as fog computing and the Internet of Things (IoT) enable efficient data sharing, while cloud computing supports large-scale healthcare analytics despite challenges like latency and

context-awareness. The concept of "autonomous cities" integrates AI, deep learning, big data, and IoT to promote sustainable and smart healthcare solutions. With a growing aging population, researchers and industries are prioritizing intelligent healthcare systems and innovative applications (Junaid et al., 2022).Hybrid intelligent systems, which combine computational techniques like genetic algorithms, CNNs, LSTM, and deep belief networks, are transforming decision-making, remote monitoring, medical logistics, and diagnostics. In biomedical engineering, these systems automate processes, improve disease detection, and function as clinical decision support tools (CDSS) for physicians (Siala et al., 2022). Soft computing methods further assist in classifying disease states, though achieving human-level accuracy remains a challenge. Machine learning plays a critical role in analyzing large historical datasets, allowing systems to learn patterns through specialized algorithms and improve predictive accuracy. This capability is essential for modern healthcare, where efficient and reliable disease detection is increasingly in demand**.**

3.0METHODOLOGICAL FRAMEWORK

The Hybrid XGBoost–IT2FLS workflow (Figure 1) follows a structured process to improve prediction accuracy and interpretability in prostate cancer analytics. It begins with the Knowledge Base, which stores rules, patient data, symptoms, and treatments. Clinical inputs such as PSA levels, demographics, and biopsy results are extracted and preprocessed through cleaning, feature selection, and normalization. The Hybrid Modeling phase integrates XGBoost for robust prediction and feature importance with IT2FLS to handle uncertainty using fuzzy rules, ensuring both accuracy and explainability. Model performance is validated using metrics like accuracy, precision, recall, F1-score, and ROC-AUC, with iterative refinements as needed. Finally, the optimized hybrid engine is deployed in clinical systems, delivering real-time, interpretable predictions and continuously improving as new data updates the Knowledge Base

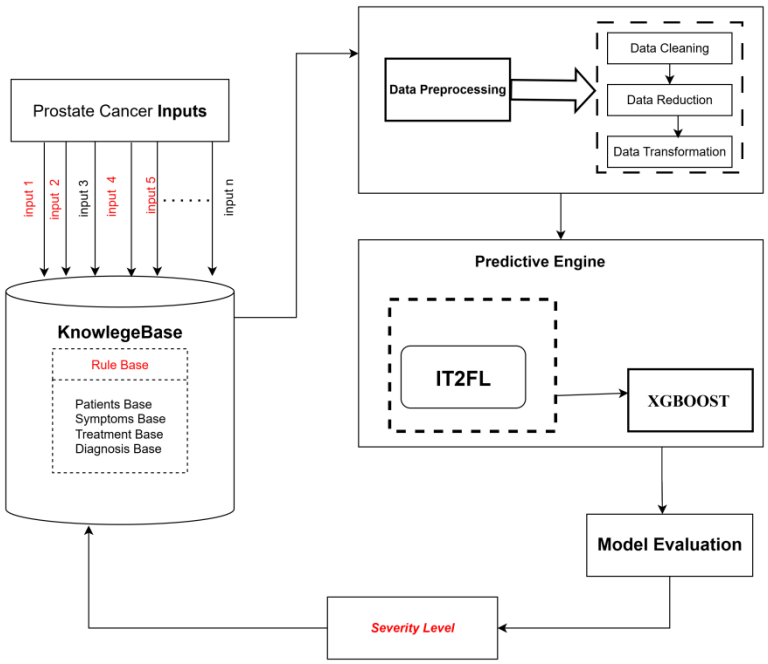


Figure 1: Conceptual diagram for a Hybrid IT2FL-XGBOOST Approach for Prostate Cancer Analytics

4.0 EXPERIMENTATION AND ANALYSIS

4.1 Data Collection and Description

The dataset used for this study, *prostate_cancer_prediction.csv*, contains 27,945 records and 30 attributes, including 24 categorical and 6 numerical variables. These features collectively provide a robust foundation for accurate prediction and prognosis. The categorical attributes capture essential diagnostic details such as patient history and medical conditions, while the numerical attributes offer critical quantitative measures that enhance predictive performance, as summarized in Table 1.

Table 1: Descriptive Statistics of the Hybrid System Dataset for Prostate Cancer Detection and Prognosis

Dataset Name	Dataset Size		Features	
	Rows	Columns	Categorical	Numeric
prostate_cancer_prediction.csv	27945	30	24	6

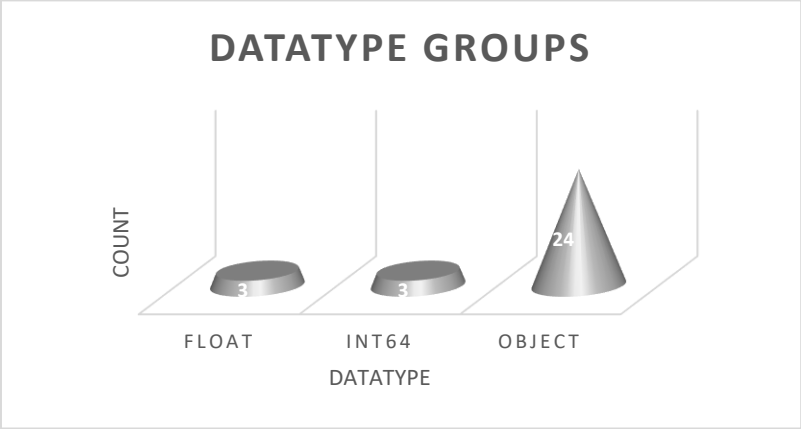


Figure 2: Datatype statistics for Prostate Cancer Detection and Prognosis

The prostate cancer dataset consists of key numerical features, with their descriptive statistics summarized in Table 2. These include Age, PSA_Level, BMI, Screening_Age, and Prostate_Volume. The dataset contains 27,945 records, where Age ranges from 40 to 89 years (mean: 64.46; SD: 14.40), indicating a broad age distribution among patients. PSA_Level, a vital marker for cancer detection, averages 7.75 ng/mL within a range of 0.5 to 15 ng/mL, with higher values often associated with increased cancer risk. BMI varies between 18 and 35 (mean: 26.51), reflecting diverse health conditions. Screening_Age shows an average of 56.90 years, aligning with typical initial screening periods. Prostate_Volume spans 15 to 80 cc, with a mean of 47.76 cc, illustrating differences in prostate size. These numerical indicators, combined with categorical features, form a robust basis for building accurate predictive models for early detection and prognosis.

Table 2: Descriptive Statistics of Numerical Features for Prostate Cancer Detection and Prognosis

Statistics	Patient_ID	Age	PSA_Level	BMI	Screening_Age	Prostate_Volume
count	27945	27945	27945	27945	27945	27945
mean	13973	64.45993917	7.751599213	26.5116	56.90230811	47.75577026
std	8067.170973	14.40475521	4.175011539	4.888293	10.11806432	18.70428607
min	1	40	0.5	18	40	15
25%	6987	52	4.13	22.3	48	31.7
50%	13973	64	7.75	26.5	57	47.7
75%	20959	77	11.32	30.7	66	63.9
max	27945	89	15	35	74	80

The prostate cancer dataset includes several numerical variables with important statistical characteristics, as mentioned in Table 3. Skewness values for Age (0.0158), PSA Level (0.0009), BMI (0.0017), and Screening Age (0.0138) are close to zero, indicating approximately symmetric distributions. Negative kurtosis values suggest relatively flat distribution curves across these variables. Among all features, Patient_ID shows the highest variance (6.51E+07) and standard deviation (8067.171), signifying a broad numeric spread. For clinical attributes, Prostate Volume displays the greatest variability, with a variance of 350 and a standard deviation of 18.70. These measures provide essential insights into data distribution and variability, supporting normality assessment and the development of robust predictive models.

Table 3: Key Statistical Measures for Numerical Features in Prostate Cancer Dataset

Feature	Skewness	Kurtosis	Variance	Standard Deviation
Patient_ID	0	-1.2	6.51E+07	8067.171
Age	0.015776	-1.19409	2.07E+02	14.40476
PSA_Level	0.000907	-1.19527	1.74E+01	4.175012
BMI	0.001722	-1.19307	2.39E+01	4.888293
Screening_Age	0.013817	-1.20681	1.02E+02	10.11806
Prostate_Volume	-0.00653	-1.19272	3.50E+02	18.70429

4.2 Data Preprocessing

Data preprocessing is a crucial step in ensuring dataset quality and enabling accurate prostate cancer detection and prognosis. In this study, preprocessing involved handling missing values, normalizing numerical features, encoding categorical variables, and selecting the most relevant attributes. To further reduce dimensionality and eliminate redundancy, Principal Component Analysis (PCA) was employed while retaining critical information.

PCA identified three major components, as shown in Table 4, that contributed significantly to data variance. The first, PC1 (Age), accounted for the highest variance at 23.96% with an eigenvalue of 2.9335, emphasizing age as a dominant predictive factor. PC2 (Family History) contributed 8.24%, highlighting its moderate impact, while PC3 (Race – African Ancestry) explained 8.23%, indicating the role of genetic predisposition in prostate cancer risk. This dimensionality reduction improved model efficiency and interpretability without sacrificing predictive accuracy**.**

Table 4: Feature Selection Using Principal Component Analysis (PCA)

S/N	Feature	Principal Component	Eigenvalue	Explained Variance Ratio
1	Age	PC1	2.9335	0.2396
2	Family_History	PC2	1.009	0.0824
3	Race_African_Ancestry	PC3	1.007	0.0823

Figure 3 illustrates the explained variance of principal components obtained from the PCA analysis for prostate cancer detection, highlighting those with eigenvalues ≥ 1. The first component (PC1) exhibits the highest eigenvalue (~2.93) and captures the greatest proportion of variance, making it the most influential factor in the dataset. PC2 and PC3, each with eigenvalues close to 1, provide moderate contributions to feature representation. The steep drop from PC1 to PC2 indicates that most variability is explained by PC1, emphasizing its importance in dimensionality reduction. Beyond PC2, the scree plot curve flattens, showing that additional components add little value and may introduce noise. This pattern confirms that retaining only the leading components optimizes data representation, reduces redundancy, and maintains predictive accuracy. Therefore, the scree plot is essential for identifying the optimal number of components for effective modeling and interpretation in prostate cancer analytics.

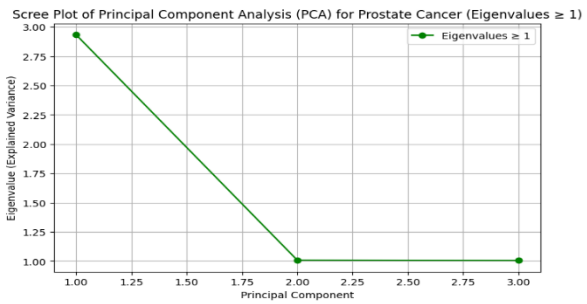


Figure 3: PCA Selection Plot

4.3 IT2FL-XGBoost Hybridization Modelling

Figure 4 represents a Type-2 Mamdani Fuzzy Inference System designed to evaluate the risk of prostate cancer based on three key input variables: Age, Family History, and African Ancestry. Each input is characterized by a set of triangular membership functions (MFs) that capture different linguistic categories. Specifically, Age and Family History are each represented by three MFs while Race_African_Ancestry is represented using two MFs, these fuzzy inputs are processed through the Mamdani Type-2 inference engine, which utilizes a rule base to infer the level of prostate cancer risk. The output, Prostate_Cancer, is defined using two MFs

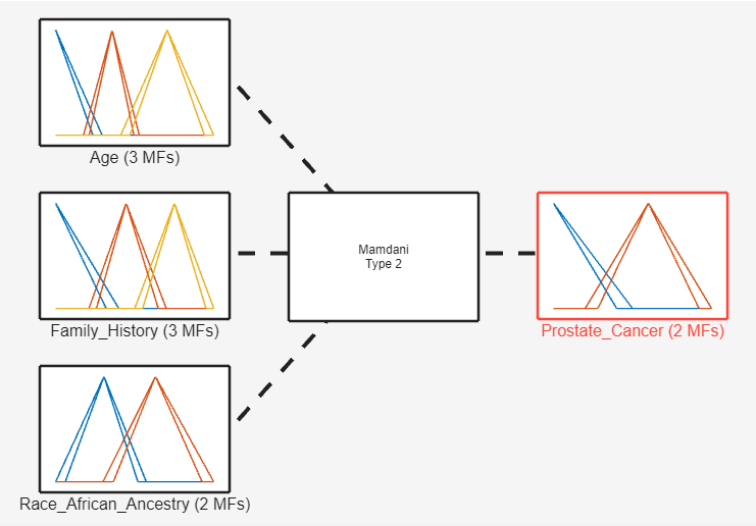


Figure 4: Fuzzy Inference System Plot

Table 5 defines the fuzzy membership functions for the input variable Age, using three linguistic terms: Young, Middle_Age, and Elderly. Each of these terms is modeled with a triangular membership function, with the upper parameters specifying the range of values that define each category. For instance, the Young category is defined by the range [15 15 40], indicating that individuals up to 40 years fall within this group, while Middle_Age spans from 30 to 60 years and Elderly from 50 to 100 years. The use of overlapping ranges enables smooth transitions between categories, accommodating the gradual nature of aging. The lower scale and lower lag values remain consistent across all categories, helping to standardize the level of fuzziness in classification.

Table 5: Fuzzy Parameter Terms for Age MF

AGE (INPUT)					
S/N	**Name**	**Type**	**Upper Parameter**	**Lower Scale**	**Lower Lag**
1	young	Traingular	[15 15 40]	1	[0.2 0.2]
2	Middle_Age	Traingular	[30 45 60]	1	[0.2 0.2]
3	Elderly	Traingular	[50 75 100]	1	[0.2 0.2]

Table 6 shows Family_History variable using two triangular membership functions: Negligible and Non-Negligible. The Negligible category is defined within the range [0 0.306104 0.573609], while the non-negligible category lies between [0.210952 0.44614 0.7]. These values represent the degree of influence that family history has on the individual's risk profile. The uniform application of the lower scale and lower lag indicates a consistent measure of uncertainty across both categories.

Table 6: Fuzzy Parameter Terms for Family_History MF

Family_History(INPUT)					
S/N	**Name**	**Type**	**Upper Parameter**	**Lower Scale**	**Lower Lag**
1	Negligible	Traingular	[0 0.306104 0.573609]	1	[0.2 0.2]

2	Non-Negligible	Traingular	[0.210952 0.44614 0.7]	1	[0.2 0.2]

Table 7 outlines the fuzzy membership functions for the input variable Race_African_Ancestry, with three linguistic terms: Absent, Partial, and Present. These are also represented using triangular functions with ranges [0 0 0.4] for Absent, [0.210952 0.44614 0.7] for Partial, and [0.5 0.751346 1.0009] for Present. These ranges are designed to capture varying degrees of African ancestry, which is a significant demographic factor in prostate cancer risk. Like other inputs, this variable uses consistent fuzziness parameters to ensure coherent behavior in the system.

Table 7: Fuzzy Parameter Terms for Race_African_Ancestry MF

Race_African_Ancestry (INPUT)					
S/N	**Name**	**Type**	**Upper Parameter**	**Lower Scale**	**Lower Lag**
1	Absent	Traingular	[0 0 0.4]	1	[0.2 0.2]
2	Partial	Traingular	[0.210952 0.44614 0.7]	1	[0.2 0.2]
3	Present	Traingular	[0.5 0.751346 1.0009]	1	[0.2 0.2]

Table 8 defined with two triangular membership functions: Negative and Positive. The Negative diagnosis is represented by the range [0 0 0.5], while Positive spans [0.2 0.6 1]. These overlapping values indicate that the model accommodates a degree of uncertainty in determining the presence or absence of cancer. The output reflects the fuzzy nature of medical diagnosis, which rarely conforms to absolute categories, especially in early detection stages.

Table 8: Fuzzy Parameter Terms for Prostate Cancer MF

Prostate Cancer(OUTPUT)					
S/N	**Name**	**Type**	**Upper Parameter**	**Lower Scale**	**Lower Lag**
1	Negative	Traingular	[0 0 0.5]	1	[0.2 0.2]
2	Positive	Traingular	[0.2 0.6 1]	1	[0.2 0.2]

4.3.1 Plot of Membership Function

Figure 5 show the input variable "Age" is divided into three linguistic categories—Young, Middle-aged, and Elderly. The "Young" category starts with full membership at age 20 and gradually declines to zero by age 40. The "Middle-aged" group begins around age 35, peaks at 50, and ends at 65, overlapping with both Young and Elderly. "Elderly" initiates from 60, reaches its peak at 75, and ends around age 90. This triangular distribution allows the fuzzy system to smoothly transition between age groups, reflecting the natural variability in age-related health risks.

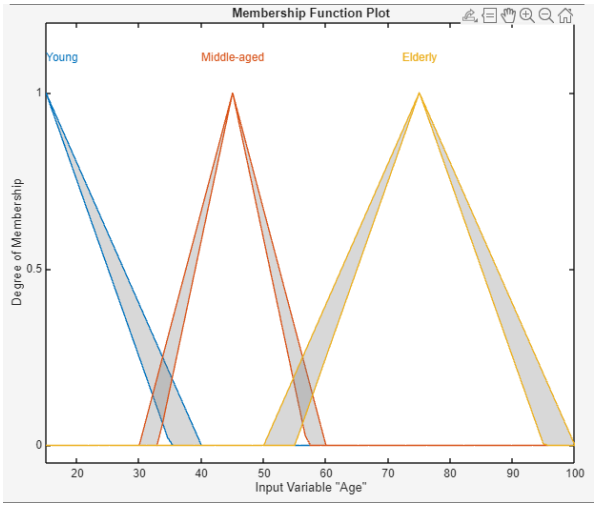


Figure 5: Membership Function Plot for Age

Figure 6 shows the input variable "Family_History" and it is characterized by three categories: Absent, Partial, and Present. The "Absent" membership begins strongly at 0 and reduces to zero by 0.3, indicating no known family history of the condition. The "Partial" classification emerges from 0.3, peaks at 0.5, and concludes at 0.7, representing individuals with limited or unclear hereditary links. Finally, "Present" starts from 0.6, peaks at 0.75, and trails off by 0.9, covering those with a strong familial predisposition. These overlapping triangular shapes allow for nuanced assessments of family history's influence on the health condition.

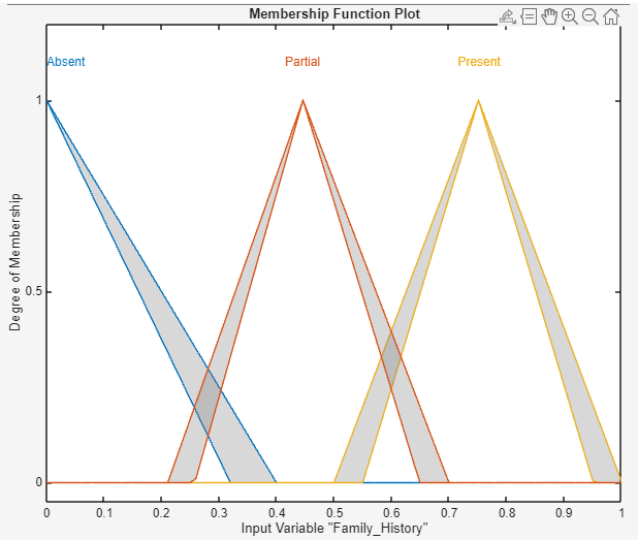


Figure 6: Membership Function Plot for Family_History

Figure 7 indicate the input variable "Race_African_Ancestry," the membership function includes two classes: Negligible and Non-Negligible. "Negligible" starts at 0, peaks sharply at 0.3, and falls to zero by 0.5, representing a minimal connection to African ancestry. "Non-Negligible" begins at 0.5, reaches a peak around 0.7, and ends at 1. This setup helps model the racial component's influence on prostate cancer risk, allowing the fuzzy system to weigh race-related susceptibility in a continuous, rather than binary, fashion.

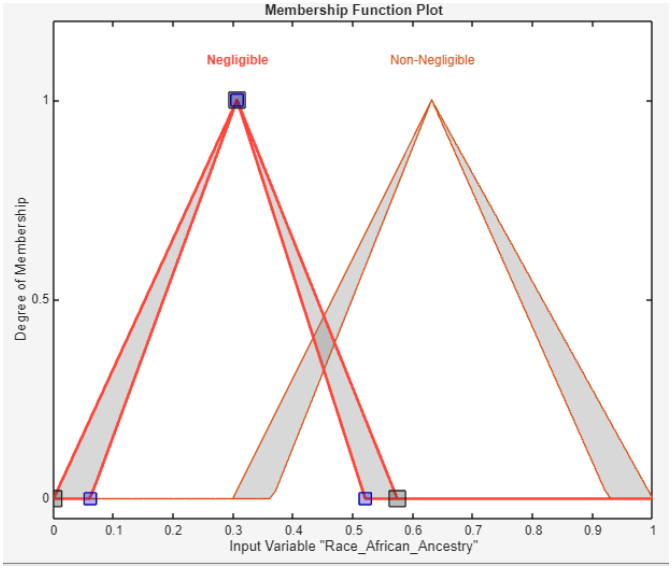


Figure 7: Membership Function Plot for Race_African Ancestry

Figure 8 indicate the output variable "Prostate_Cancer" is divided into two fuzzy sets Negative and Positive. The "Negative" class starts at 0 with maximum membership, tapering off at 0.4, indicating low to moderate risk of cancer presence. The "Positive" category starts from 0.4, peaks at 0.6, and ends at 1, indicating increasing certainty of cancer diagnosis. This overlap enables a flexible interpretation of diagnostic outcomes, accounting for borderline or uncertain cases based on fuzzy inference rather than hard thresholds.

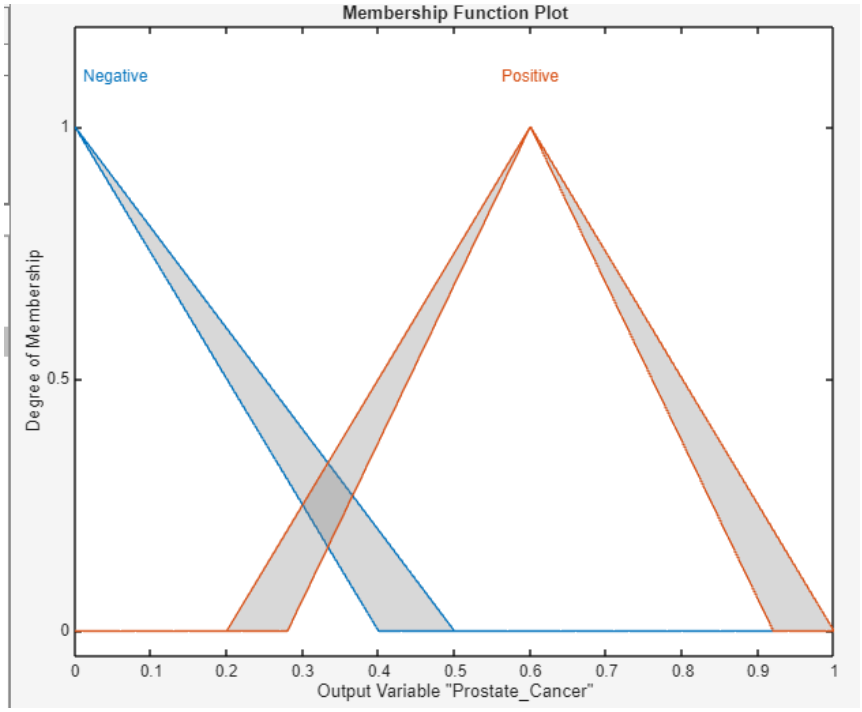


Figure 8: Membership Function Plot for Prostate Cancer

4.3.2 IT2FL Rules

Table 9 presents a set of Interval Type-2 Fuzzy Logic (IT2FL) rules designed to support the detection and prognosis of prostate cancer. Each rule integrates three antecedent variables Age, Family History, and Race (African Ancestry) to infer the likelihood of a Prostate Cancer diagnosis as either positive or negative. The rules are structured to accommodate both and/or logical operators, allowing for nuanced combinations of patient characteristics. For instance, Rule 1 asserts that if the patient is young, has no family history of prostate cancer, and is not of African ancestry, then the diagnosis is negative, while Rule 2 suggests a positive prognosis under similar conditions but with a middle-aged patient. The table incorporates all combinations across three age groups (young, middle-aged, elderly), three levels of family history (absent, partial, present), and two racial categories (negligible or non-negligible African ancestry). Each rule is assigned a weight of 1, indicating equal influence in the fuzzy inference system, and is uniquely indexed for traceability. The antecedents are numerically encoded in the form [Age, Family_History, Race], and the consequent is labeled as 1 (Negative) or 2 (Positive), offering a structured and interpretable logic-based framework to support clinical decision-making in prostate cancer assessment.

Table 9: IT2FL Rules for Prostate Cancer Detection and Prognosis

SN	Rule	Weight	Name	Antecedent	consequent
1	If Age is Young and Family_History is Absent and Race_African_Ancestry is Negligible then Prostate_Cancer is Negative	1	Rule 1	[1,1,1]	1
2	If Age is Middle-aged and Family_History is Absent and Race_African_Ancestry is Negligible then Prostate_Cancer is Positive	1	Rule 2	[2,1,1]	2
3	If Age is Elderly and Family_History is Absent and Race_African_Ancestry is Negligible then Prostate_Cancer is Negative	1	Rule 3	[3,1,1]	1
4	If Age is Young or Family_History is Partial or Race_African_Ancestry is Negligible then Prostate_Cancer is Positive	1	Rule 4	[1,2,1]	2
5	If Age is Middle-aged and Family_History is	1	Rule 5	[2,2,1]	2

	Partial and Race_African_Ancestry is Negligible then Prostate_Cancer is Positive				
6	If Age is Elderly and Family_History is Partial and Race_African_Ancestry is Negligible then Prostate_Cancer is Negative	1	Rule 6	[3,2,1]	1
7	If Age is Young and Family_History is Present and Race_African_Ancestry is Negligible then Prostate_Cancer is Negative	1	Rule 7	[1,3,1]	1
8	If Age is Middle-aged and Family_History is Present and Race_African_Ancestry is Negligible then Prostate_Cancer is Positive	1	Rule 8	[2,3,1]	2
9	If Age is Elderly and Family_History is Present and Race_African_Ancestry is Negligible then Prostate_Cancer is Negative	1	Rule 9	[3,3,1]	1
10	If Age is Young or Family_History is Absent or Race_African_Ancestry is Non-Negligible then Prostate_Cancer is Positive	1	Rule 10	[1,1,2]	2
11	If Age is Middle-aged and Family_History is Absent and Race_African_Ancestry is Non-Negligible then Prostate_Cancer is Negative	1	Rule 11	[2,1,2]	1
12	If Age is Elderly and Family_History is Absent and Race_African_Ancestry is Non-Negligible then Prostate_Cancer is Negative	1	Rule 12	[3,1,2]	1
13	If Age is Young and Family_History is Partial and Race_African_Ancestry is Non-Negligible then Prostate_Cancer is Positive	1	Rule 13	[1,1,2]	2
14	If Age is Middle-aged or Family_History is Partial or Race_African_Ancestry is Non-Negligible then Prostate_Cancer is Negative	1	Rule 14	[2,2,2]	1
15	If Age is Elderly and Family_History is Partial and Race_African_Ancestry is Non-Negligible then Prostate_Cancer is Negative	1	Rule 15	[3,2,2]	1
16	If Age is Young and Family_History is Present and Race_African_Ancestry is Non-Negligible then Prostate_Cancer is Positive	1	Rule 16	[1,3,2]	1
17	If Age is Middle-aged and Family_History is Present and Race_African_Ancestry is Non-Negligible then Prostate_Cancer is Negative	1	Rule 17	[2,3,2]	1
18	If Age is Elderly and Family_History is Present and Race_African_Ancestry is Non-Negligible then Prostate_Cancer is Positive	1	Rule 18	[3,3,2]	2

4.3.3 Firing Inference

Figure 9 and Figure 10 uses three input variables Age (60 years), Family History (0), and Race: African Ancestry (1) to evaluate 18 fuzzy rules and produce a prostate cancer risk value of 0.428. Each row in the diagram represents a rule, showing how each input matches fuzzy membership functions (like low, medium, high) using triangular shapes. The red lines indicate how the input values activate these functions. For example, the Age input at 60 partially activates both "middle-aged" and "old" fuzzy sets, while Family History being 0 only activates the "No history" set, and Race being 1 fully activates "African Ancestry." The system applies fuzzy logic (AND/OR) to combine inputs per rule and calculates how strongly each rule is triggered. The more a rule matches the inputs, the more it contributes to the final output. The output column on the right

shows how all rules combine to estimate the risk of prostate cancer, which, in this case, is moderately high at 0.428, mainly influenced by Age and Race, while the absence of family history lowers the risk slightly.

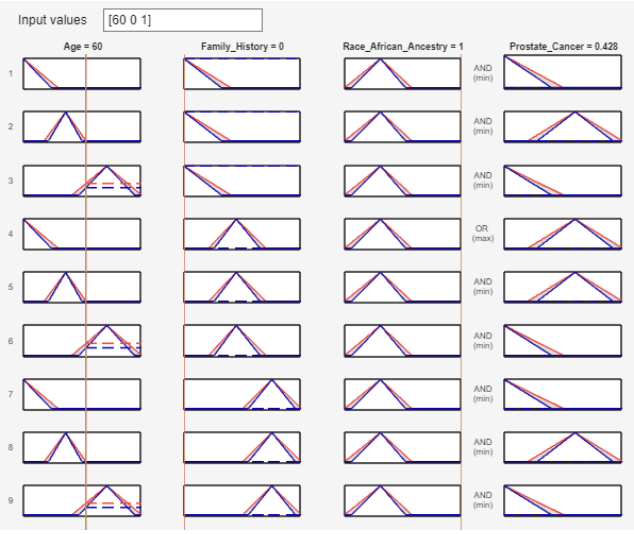


Figure 9(a): Firing Inference(a)

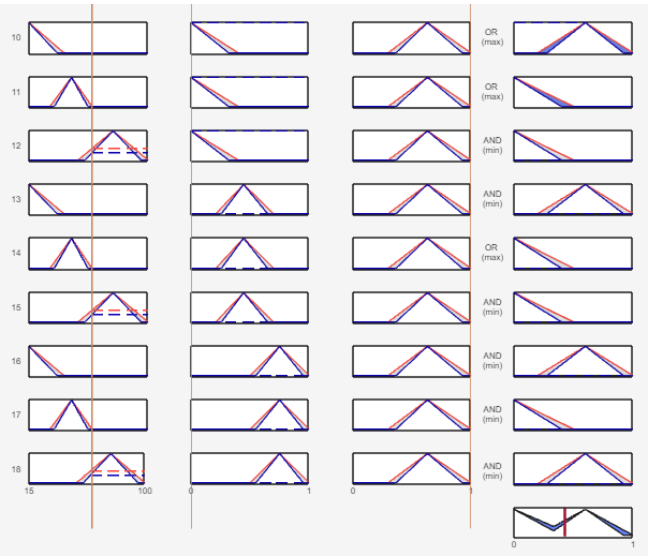


Figure 10(b): Firing Inference

In this Hybrid Model ,Reference Output was gotten from IT2FL which is feed as input to XGBoot and the result gotten is shown in Table 10. Table 10 presents The classification results indicate strong overall model performance, with an accuracy of 97% across 5,589 test samples. For the No class, the model achieved a precision of 0.97, recall of 0.83, and F1-score of 0.89 based on 994 samples, indicating that while most predicted No cases were correct, the model missed some actual No cases. For the Yes class, the model obtained a precision of 0.96, recall of 0.99, and F1-score of 0.98 across 4,595 samples, demonstrating highly effective identification of Yes cases. The macro-average precision, recall, and F1-score were 0.97, 0.91, and 0.94, respectively, while the weighted-average values were 0.97, 0.97, and 0.96. The difference between the macro and weighted averages reflects the unequal class distribution, with substantially more Yes than No observations. Overall, the model performs strongly, although its lower recall for the No class suggests some difficulty in correctly identifying negative cases.

Table 10: Classification Report for IT2FL-XGBoost Model

Class / Average	Precision	Recall	F1-Score	Support
No	0.97	0.83	0.89	994

Yes	0.96	0.99	0.98	4,595
Accuracy	—	—	**0.97**	5,589
Macro Average	0.97	0.91	0.94	5,589
Weighted Average	0.97	0.97	0.96	5,589

This matrix evaluates the diagnostic accuracy of the hybrid model on the test dataset as in Figure 11. The model demonstrates high efficacy in identifying prostate cancer cases, correctly classifying 4,567 instances as "Yes" (True Positives) and 827 instances as "No" (True Negatives). The relatively low number of false negatives (28) is particularly critical in cancer analytics, as it indicates the model is highly sensitive and unlikely to miss a patient who actually has the disease. The 167 false positives represent cases where the model predicted cancer but the patient was healthy; while this requires further testing, it is a safer error than a missed diagnosis.

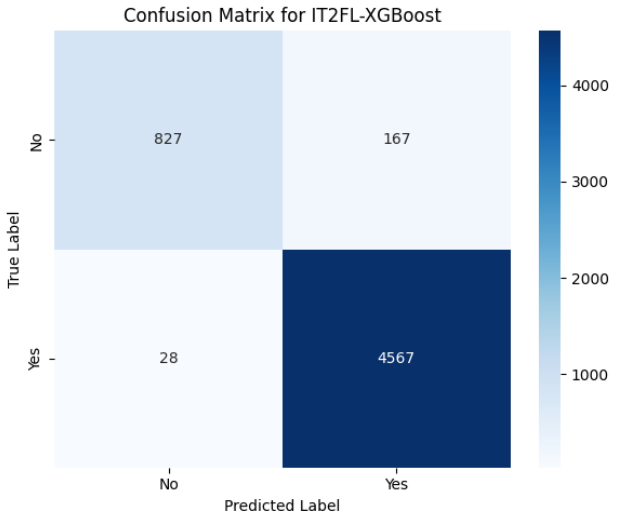


Figure 11: Confusion Metrics for IT2FL-XGBoost

This bar chart illustrates the relative contribution of input variables to the decision-making process of the XGBoost classifier as in Figure 12. The chart indicates that RefOutput is the overwhelmingly dominant feature, with an importance score of approximately 414. In the context of this hybrid approach, this suggests that the specific output generated by the Type-2 Fuzzy Logic (IT2FL) system—likely a risk score or a linguistic variable derived from clinical data—is the primary driver for the final classification. This validates the "hybrid" nature of the approach, showing that the fuzzy logic component provides the most critical information for the analytics.

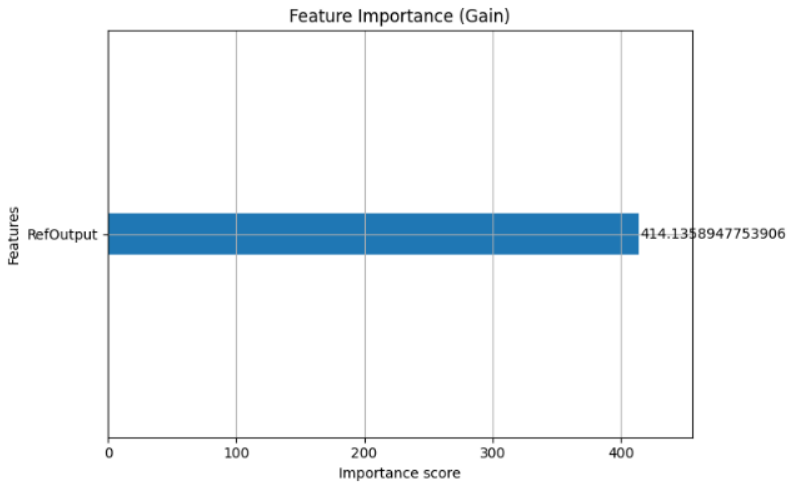


Figure 12: Feature Importance (Gain)

Figure 12 shows This learning curve tracks the model's error rate (Logloss) over 300 training iterations. The curve shows a rapid decrease in error within the first 50 iterations, followed by a plateau near 0.15. This indicates that the IT2FL-XGBoost model converges quickly and efficiently. The stability of the curve suggests that the model is not overfitting and has successfully learned the underlying patterns in the prostate cancer data without significant variance in the later epochs.

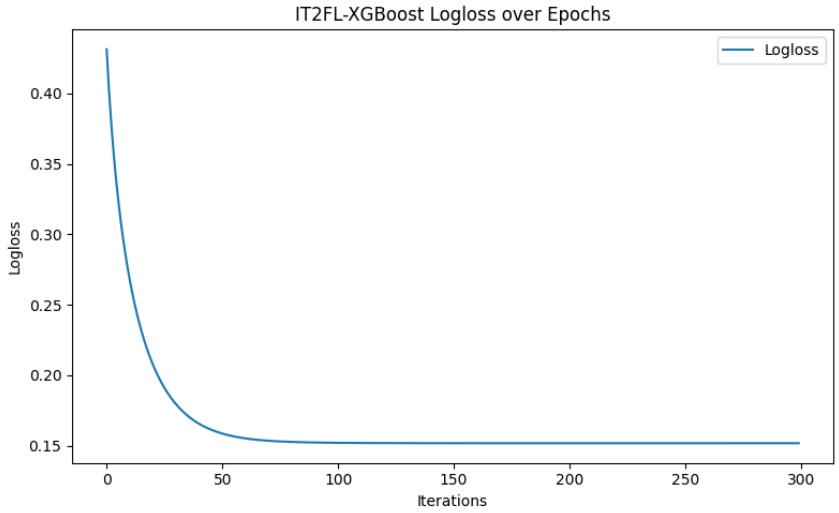


Figure 13: Logloss for IT2FL-XGBoost

Figure 13 provides a look into the internal logic of a single decision tree within the XGBoost ensemble. It shows a simple split based on the feature **RefOutput**. If the value of RefOutput is less than 1, the model follows the "yes" branch to a leaf value of -0.266, pushing the prediction toward a negative class. Conversely, if the value is greater than or equal to 1, it follows the "no, missing" branch to a positive leaf value of 0.046. This visualizes how the model creates non-linear boundaries to separate cancerous from non-cancerous cases based on the fuzzy logic inputs.

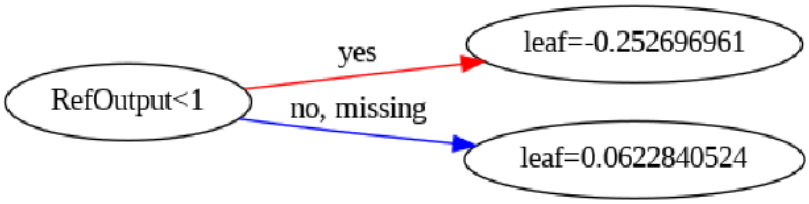


Figure 14: IT2FL-XGBoost Tree Diagram

Figure 14 demonstrates that The SHAP (SHapley Additive exPlanations) summary plot offers explainability regarding the "RefOutput" feature. It clearly separates the data into two distinct clusters: high feature values (pink) have a strong positive impact on the model output (pushing predictions toward "Cancer"), while low feature values (blue) have a negative impact. This confirms the global explainability of the model, ensuring that the "black box" of XGBoost can be interpreted by clinicians—high values of the fuzzy logic output are mathematically proven to drive the diagnosis of prostate cancer.

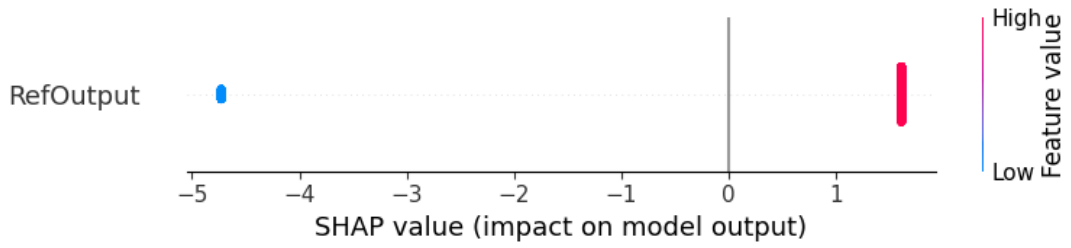


Figure 14: Plot of Feature Contributions for IT2FL-XGBoost

Figure 15 illustrates The reliability diagram assesses the probabilistic trustworthiness of the model. The "Calibrated XGBoost" line (blue squares) follows the "Perfect Calibration" diagonal line (black dashed) almost exactly. This signifies that the model's predicted probabilities are realistic; for example, when the model predicts a 70% chance of cancer, the patient effectively has a 70% chance of having the disease. In a clinical setting, this ensures that doctors can trust the confidence scores provided by the IT2FL-XGBoost system for making informed treatment decisions.

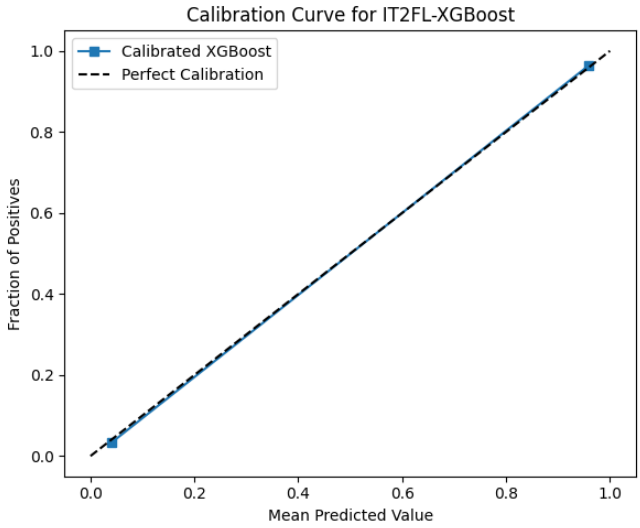


Figure 15: Calibration Curve for IT2FL-XGBoost

5.0 RESULTS AND DISCUSSION

The fuzzy inference system uses three primary input variables—Age, Family History, and Race (African Ancestry) and applies 18 expert-defined fuzzy rules to model uncertainty in prostate cancer risk assessment. The rules represent clinical variables using linguistic terms and generate an interpretable risk decision of Yes/No. By incorporating uncertainty through interval type-2 fuzzy sets, the system provides a transparent representation of ambiguous patient characteristics and supports interpretable risk assessment. The resulting fuzzy-based representations are subsequently used by the machine learning model to improve classification performance. The evaluation results demonstrate strong classification performance, with an overall accuracy of 0.97 across 5,589 test samples. For the No class, the model achieved a precision of 0.97, recall of 0.83, and F1-score of 0.89 from 994 samples, indicating that most predicted No cases were correctly classified, although some actual No cases were classified as Yes. For the Yes class, the model achieved a precision of 0.96, recall of 0.99, and F1-score of 0.98 across 4,595 samples, demonstrating highly effective identification of prostate cancer-positive cases. The macro-average precision, recall, and F1-score were 0.97, 0.91, and 0.94, respectively, while the weighted-average precision, recall, and F1-score were 0.97, 0.97, and 0.96. These results indicate that the hybrid model provides strong predictive performance across both classes, with particularly high sensitivity for identifying positive cases, while the comparatively lower recall for the No class indicates an area for further improvement.

6.0 CONCLUSION

This study introduced a hybrid model combining Interval Type-2 Fuzzy Logic (IT2FL) with XGBoost to support prostate cancer risk classification under uncertainty. The IT2FL component captures uncertainty in clinical variables through expert-defined fuzzy rules, while XGBoost provides data-driven predictive capability. The integration of both approaches produces an interpretable classification framework that combines fuzzy reasoning with machine learning. The evaluation results showed an overall accuracy of 97%, with precision, recall, and F1-score of 0.97, 0.83, and 0.89, respectively, for the No class, and 0.96, 0.99, and 0.98 for the Yes class. The weighted-average precision, recall, and F1-score were 0.97, 0.97, and 0.96, respectively. These findings indicate strong predictive performance, particularly in identifying positive cases, while the lower recall for the No class highlights an opportunity for further model refinement. By combining

uncertainty-aware fuzzy reasoning with machine learning, the proposed approach provides both predictive capability and interpretability, making it a potentially useful decision-support framework for prostate cancer risk assessment.

REFERENCES

1. Ahmed, H. U., El-Shater Bosaily, A., Brown, L. C., Gabe, R., Kaplan, R., Parmar, M. K., & Emberton, M. (2017). Diagnostic accuracy of multi-parametric MRI and TRUS biopsy in prostate cancer (PROMIS): A paired validating confirmatory study. The Lancet, 389(10071), 815–822. https://doi.org/10.1016/s0140-6736(16)32401-1
2. Bhattacharya, I., Khandwala, Y. S., Vesal, S., Shao, W., Yang, Q., Soerensen, S. J., Fan, R. E., Ghanouni, P., Kunder, C. A., Brooks, J. D., Hu, Y., Rusu, M., & Sonn, G. A. (2022). A review of artificial intelligence in prostate cancer detection on imaging. Therapeutic Advances in Urology, 14, 175628722211287. https://doi.org/10.1177/17562872221128791
3. Chervenkov, L., Sirakov, N., Kostov, G., Velikova, T., & Hadjidekov, G. (2023). Future of prostate imaging: Artificial intelligence in assessing prostatic magnetic resonance imaging. World Journal of Radiology, 15(5), 136–145. https://doi.org/10.4329/wjr.v15.i5.136
4. Cuocolo, R., Cipullo, M. B., Stanzione, A., Romeo, V., Green, R., Cantoni, V., Ponsiglione, A., Ugga, L., & Imbriaco, M. (2020). Machine learning for the identification of clinically significant prostate cancer on MRI: a meta-analysis. European Radiology, 30(12), 6877–6887. https://doi.org/10.1007/s00330-020-07027-w
5. Cuocolo, R., Comelli, A., Stefano, A., Benfante, V., Dahiya, N., Stanzione, A., Castaldo, A., De Lucia, D. R., Yezzi, A., & Imbriaco, M. (2021). Deep learning Whole-Gland and zonal prostate segmentation on a public MRI dataset. Journal of Magnetic Resonance Imaging, 54(2), 452–459. https://doi.org/10.1002/jmri.27585
6. DeSantis, C. E., Miller, K. D., Goding Sauer, A., Jemal, A., & Siegel, R. L. (2019). Cancer statistics for African Americans, 2019. CA: A Cancer Journal for Clinicians, 69(3), 211–233. https://doi.org/10.3322/caac.21555
7. Ge, A., Chang, Z., & Feng, J. E. (2023). Interval Type-2 fuzzy relation matrix model via semitensor product. IEEE Transactions on Fuzzy Systems, 31(11), 3984–3994. https://doi.org/10.1109/tfuzz.2023.3273215
8. Hiremath, A., Shiradkar, R., Fu, P., & et al. (2021). An integrated nomogram combining deep learning, prostate imaging–reporting and data system (PI-RADS) scoring, and clinical variables for identification of clinically significant prostate cancer on biparametric MRI: A retrospective multicentre study. Lancet Digital Health, 3(6), e445–e454. https://doi.org/10.1016/S2589-7500(21)00125-6
9. Iheanacho, C. and Enechukwu, O. (2024). Epidemiology of prostate cancer in Nigeria: a mixed methods systematic review.. Cancer causes & control : CCC. https://doi.org/10.1007/s10552-024-01917-w
10. Junaid, S. B., Imam, A. A., Balogun, A. O., De Silva, L. C., Surakat, Y. A., Kumar, G., Abdulkarim, M., Shuaibu, A. N., Garba, A., Sahalu, Y., Mohammed, A., Mohammed, T. Y., Abdulkadir, B. A., Abba, A. A., Kakumi, N. A. I., & Mahamad, S. (2022). Recent advancements in emerging technologies for healthcare management systems: A survey. Healthcare, 10(10), 1940. https://doi.org/10.3390/healthcare10101940
11. Kohaar, I., Petrovics, G., & Srivastava, S. (2019). A rich array of prostate cancer molecular biomarkers: Opportunities and challenges. International Journal of Molecular Sciences, 20(8), 1813. https://doi.org/10.3390/ijms20081813
12. Leyh-Bannurah, S. R., Karakiewicz, P. I., Pompe, R. S., Preisser, F., Zaffuto, E., Dell'Oglio, P., & Budäus, L. (2018). Inverse stage migration patterns in North American patients undergoing local prostate cancer treatment: A contemporary population-based update in light of the 2012 USPSTF recommendations. World Journal of Urology, 37(3), 469–479. https://doi.org/10.1007/s00345-018-2396-2
13. Liu, P., Jin, K., Jiao, Y., He, M., & Fei, S. (2021). Prediction of second primary lung cancer patient's survivability based on improved Eigenvector Centrality-Based Feature selection. IEEE Access, 9, 55663–55672. https://doi.org/10.1109/access.2021.3063944

14. Negoita, S., Feuer, E. J., Mariotto, A., Cronin, K. A., Petkov, V. I., Hussey, S. K., & Penberthy, L. (2018). Annual report to the nation on the status of cancer, part II: Recent changes in prostate cancer trends and disease characteristics. Cancer, 124(13), 2801–2814. https://doi.org/10.1002/cncr.31549
15. Pandey, M. S., Pandey, B. N., Soam, S., Tripathi, S. P., & Mishra, A. K. (2023). A novel technique for efficient diagnosis of diseases. https://doi.org/10.22541/au.168533109.96415820/v1
16. Pandey, M. S., Pandey, B. N., Soam, S., Tripathi, S. P., & Mishra, A. K. (2023). A novel technique for efficient diagnosis of diseases. https://doi.org/10.22541/au.168533109.96415820/v1
17. Paul, M., Maglaras, L., Ferrag, M. A., & Almomani, I. (2023). Digitization of healthcare sector: A study on privacy and security concerns. ICT Express, 9(4), 571–588. https://doi.org/10.1016/j.icte.2023.02.007
18. Siala, H., & Wang, Y. (2022). SHIFTing artificial intelligence to be responsible in healthcare: A systematic review. Social Science & Medicine, 296, 114782. https://doi.org/10.1016/j.socscimed.2022.114782
19. Siegel, R. L., Miller, K. D., & Jemal, A. (2020). Cancer statistics, 2020. CA: A Cancer Journal for Clinicians, 70(1), 7–30. https://doi.org/10.3322/caac.21590
20. Siegel, R. L., Miller, K. D., Fuchs, H. E., & Jemal, A. (2022). Cancer statistics, 2022. CA: A Cancer Journal for Clinicians, 72(1), 7–33. https://doi.org/10.3322/caac.21708
21. Taye, M. M. (2023). Theoretical understanding of convolutional neural network: Concepts, architectures, applications, future directions. Computation, 11(3), 52. https://doi.org/10.3390/computation11030052
22. Turkbey, B., Rosenkrantz, A. B., Haider, M. A., & et al. (2019). Prostate imaging reporting and data system version 2.1: 2019 update of prostate imaging reporting and data system version 2. European Urology, 76(3), 340–351. https://doi.org/10.1016/j.eururo.2019.03.036
23. Umoh, U., Eyoh, I., Isong, E., Ekong, A., & Peter, S. (2020). Using interval type-2 fuzzy logic to analyze Igbo emotion words. 1(3), 217–240. https://doi.org/10.22105/jfea.2020.251544.1021
24. Umoh, U., Inyang, U. G., & Nyoho, E. E. (2019). Interval Type-2 Fuzzy Logic for Fire Outbreak Detection. International Journal on Soft Computing Artificial Intelligence and Applications, 8(3), 27–46. https://doi.org/10.5121/ijscai.2019.8303
25. Wang, N. N., Zhou, S. R., Chen, L., & et al. (2021). The Stanford prostate cancer calculator: Development and external validation of online nomograms incorporating PI-RADS scores to predict clinically significant prostate cancer. Urologic Oncology, 39(12), 831.e19–831.e27. https://doi.org/10.1016/j.urolonc.2021.07.017